

Surface states modulated exchange interaction in Bi_2Se_3/thulium iron garnet heterostructures

Hai-Bin Shi(石海滨), Li-Qin Yan(闫丽琴), Yang-Tao Su(苏仰涛), Li Wang(王力), Xin-Yu Cao(曹昕宇), Lin-Zhu Bi(毕林竹), Yang Meng(孟洋), Yang Sun(孙阳), Hong-Wu Zhao(赵宏武)

Citation: Chin. Phys. B . 2020, 29(11): 117302 . **doi:** 10.1088/1674-1056/abbbdf
Journal homepage: http://cpb.iphy.ac.cn; http://iopscience.iop.org/cpb

What follows is a list of articles you may be interested in

Improved electrical properties of NO-nitrided SiC/SiO_2 interface after electron irradiation

Ji-Long Hao(郝继龙), Yun Bai(白云), Xin-Yu Liu(刘新宇), Cheng-Zhan Li(李诚瞻), Yi-Dan Tang(汤益丹), Hong Chen(陈宏), Xiao-Li Tian(田晓丽), Jiang Lu(陆江), Sheng-Kai Wang(王盛凯)

Chin. Phys. B . 2020, 29(9): 097301 . **doi:** 10.1088/1674-1056/ab9434

High-mobility SiC MOSFET with low density of interface traps using high pressure microwave plasma oxidation

Xin-Yu Liu(刘新宇), Ji-Long Hao(郝继龙), Nan-Nan You(尤楠楠), Yun Bai(白云), Yi-Dan Tang(汤益丹), Cheng-Yue Yang(杨成樾), Sheng-Kai Wang(王盛凯)

Chin. Phys. B . 2020, 29(3): 037301 . **doi:** 10.1088/1674-1056/ab68c0

Scanning tunneling microscopic investigation on morphology of magnetic Weyl semimetal $YbMnBi_2$

Zhen Zhu(朱朕), Dong Yan(严冬), Xiao-Ang Nie(聂晓昂), Hao-Ke Xu(徐豪科), Xu Yang(杨旭), Dan-Dan Guan(管丹丹), Shiyong Wang(王世勇), Yao-Yi Li(李耀义), Canhua Liu(刘灿华), Jun-Wei Liu(刘军伟), Hui-Xia Luo(罗惠霞), Hao Zheng(郑浩), Jin-Feng Jia(贾金锋)

Chin. Phys. B . 2019, 28(7): 077302 . **doi:** 10.1088/1674-1056/28/7/077302

Strong perpendicular magnetic anisotropy in $Co_2FeAl_{0.5}Si_{0.5}$ film sandwiched by MgO layers

Wang Sheng, Li Xiao-Qi, Bai Li-Juan, Xu Xiao-Guang, Miao Jun, Jiang Yong

Chin. Phys. B . 2013, 22(5): 057305 . **doi:** 10.1088/1674-1056/22/5/057305

Magnetic properties of a Pt/Co_2FeAl/MgO structure with perpendicular magnetic anisotropy

Li Xiao-Qi, Xu Xiao-Guang, Wang Sheng, Wu Yong, Zhang De-Lin, Miao Jun, Jiang Yong

Chin. Phys. B . 2012, 21(10): 107307 . **doi:** 10.1088/1674-1056/21/10/107307

RAPID COMMUNICATION

Surface states modulated exchange interaction in Bi_2Se_3/thulium iron garnet heterostructures*

Hai-Bin Shi(石海滨)[1,2], Li-Qin Yan(闫丽琴)[1,2], Yang-Tao Su(苏仰涛)[1,2], Li Wang(王力)[1,2], Xin-Yu Cao(曹昕宇)[1,2], Lin-Zhu Bi(毕林竹)[1,2], Yang Meng(孟洋)[1,2], Yang Sun(孙阳)[1,2], and Hong-Wu Zhao(赵宏武)[1,2,3,†]

[1] *Beijing National Laboratory for Condensed Matter Physics, Institute of Physics, Chinese Academy of Sciences, Beijing* 100190, *China*
[2] *School of Physical Sciences, University of Chinese Academy of Sciences, Beijing* 100049, *China*
[3] *Songshan Lake Materials Laboratory, Dongguan* 523808, *China*

(Received 12 August 2020; revised manuscript received 16 September 2020; accepted manuscript online 28 September 2020)

We investigate the modulation of magnetic anisotropy of thulium iron garnet (TmIG) films by interfaced Bi_2Se_3 thin films. High quality epitaxial growth of Bi_2Se_3 films has been achieved by molecular beam epitaxy on TmIG films. By the method of ferromagnetic resonance, we find that the perpendicular magnetic anisotropy (PMA) of TmIG can be greatly strengthened by the adjacent Bi_2Se_3 layer. Moreover, the competition between topological surface states and thickness dependent bulk states of Bi_2Se_3 gives rise to the modulation of PMA of the Bi_2Se_3/TmIG heterostructures. The interfacial interaction can be attributed to the enhanced exchange coupling between Fe^{3+} ions of TmIG mediated by topological surface electrons of Bi_2Se_3.

Keywords: topological surface states, interfacial exchange coupling, perpendicular magnetic anisotropy

PACS: 73.20.–r, 75.70.Cn, 75.30.Et, 75.30.Gw **DOI:** 10.1088/1674-1056/abbbdf

1. Introduction

Topological insulators (TIs) are a class of quantum materials possessing nontrivial surface states, wherein the electron spin is locked orthogonally to its momentum in the film plane, leading to a robust spin–orbit coupling (SOC).[1] When TIs are contacted with a ferromagnet (FM), magnetic ordering can be introduced into the topological surface states (TSSs) via magnetic proximity effect (MPE),[2,3] which can lead to novel phenomena such as quantum anomalous Hall effect,[4] topological magnetoelectric effect,[5] etc. On the other hand, TI can also influence magnetic properties of FM through interfacial exchange coupling. It has been reported that the magnetic properties of in-plane magnetized films such as yttrium iron garnet (YIG) can be greatly modulated by the adjacent TI layer, in which TSSs play a crucial role.[2,6–9] Specifically, the spins of TI are assumed to lie in the plane due to the strong spin–momentum locking,[10] which even modifies the spin direction of YIG through exchange coupling and induces additional in-plane anisotropy.[8] For FMs with perpendicular magnetic anisotropy (PMA), the interfacial exchange coupling between FM and TI may be quite different, where the spins are perpendicular to the spins of TSSs in TIs, leading to a weaker Heisenberg-like interaction. Recently, Chen *et al.* observed that the interfacial exchange interaction in Bi_2Se_3/thulium iron garnet (TmIG) induces a large interfacial in-plane magnetic anisotropy (IMA).[11] Nevertheless, the influence of TI on the PMA of FMs has not been systematically studied yet, and it is still unclear how the TSSs participate in the interfacial interaction.

In this study, we investigate the magnetic anisotropy of TmIG/Bi_2Se_3 heterostructures. We find that the PMA of TmIG can be greatly modulated by the adjacent Bi_2Se_3 layer using ferromagnetic resonance (FMR). Moreover, the competition between TSSs and thickness dependent bulk states of Bi_2Se_3 results in the modulation of PMA of Bi_2Se_3/TmIG heterostructures. The interfacial interaction can be attributed to the strengthened exchange coupling between Fe^{3+} ions of TmIG mediated by TSS electrons of Bi_2Se_3.

2. Experimental details

High-quality single-crystal TmIG films were prepared by rf magnetron sputtering at room temperature followed by a post-annealing process. First, the stoichiometric TmIG target was cleaned and pre-sputtered. TmIG films were grown on (111)-oriented $Gd_3Ga_5O_{12}$ (GGG) substrates at the rf power of 40 W and the Ar pressure of 3.5 mTorr. Then, the TmIG films were annealed at 800 °C for 3 hours in oxygen atmosphere. The crystalline structure and magnetic properties of the TmIG films were investigated by x-ray diffraction (XRD) and the vibrating sample magnetometer (VSM), respectively. Figure 1(a) shows a 2θ–ω XRD spectrum of a TmIG film (22 nm thickness) on GGG(111), exhibiting distinct Laue

*Project supported by the National Key Basic Research Project of China (Grant No. 2016YFA0300600), the Strategic Priority Research Program of the Chinese Academy of Sciences (Grant No. XDB33020300), and the National Natural Science Foundation of China (Grant Nos. 11604375 and 11874416).

†Corresponding author. E-mail: hwzhao@iphy.ac.cn

© 2020 Chinese Physical Society and IOP Publishing Ltd

patterns and indicating excellent crystallinity of TmIG. Figure 1(b) shows the magnetic hysteresis loops with out-of-plane and in-plane applied magnetic fields, respectively. The considerably smaller coercivity and higher remanent magnetization for the out-of-plane M–H loop indicate that the TmIG film exhibits obvious PMA. To avoid discrepancy between the magnetic properties of TmIG, a series of TmIG films with the same thickness (12 nm) were prepared under the same condition in one batch. After annealing, the TmIG/GGG films were immediately transferred into an MBE chamber with a base pressure of 3.0×10^{-10} Torr, and degassed at 150 °C for 8 hours prior to Bi_2Se_3 growth. The streaky reflection high-energy electron diffraction (RHEED) pattern from the degassed TmIG surface further demonstrates the good crystallinity and smoothness of TmIG, as shown in Fig. 1(c). Thereafter, Bi_2Se_3 films (4–18 nm) were epitaxially grown on TmIG at 250 °C. The thickness of Bi_2Se_3 was monitored by a quartz crystal microbalance. The sharp and streaky RHEED pattern of a typical Bi_2Se_3 film (8 nm) is displayed in Fig. 1(d), revealing the high quality of the epitaxial growth. The good crystallinity of Bi_2Se_3 was further confirmed by Raman spectrum.

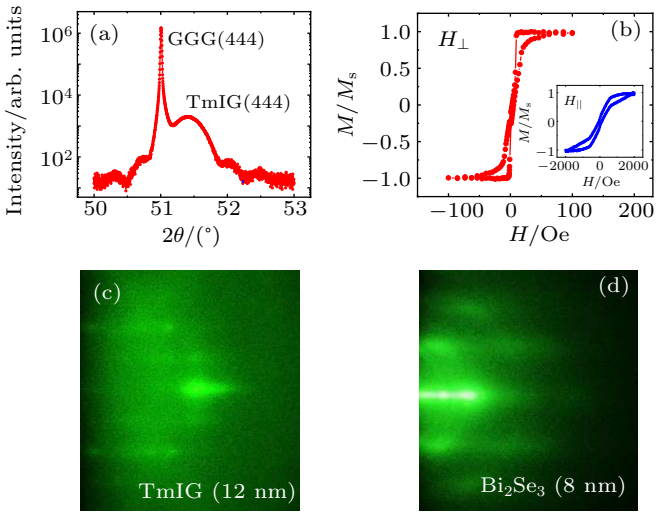


Fig. 1. (a) The 2θ–ω XRD scan of a TmIG (22 nm) film. (b) Hysteresis loop of a TmIG film (35 nm) with out-of-plane applied field. Inset: the in-plane hysteresis loop. (c) RHEED patterns of TmIG (12 nm), and (d) Bi_2Se_3 (8 nm)/TmIG (12 nm).

3. Results

3.1. Bi_2Se_3 thickness dependence study

The FMR measurements were conducted on a JEOL JES-FA200 ESR spectrometer with a 9.3-GHz microwave cavity. Figure 2(a) shows the derivative FMR spectrum of TmIG (12 nm)/Bi_2Se_3 (6 nm) obtained in out-of-plane magnetic field at room temperature. Compared with the bare TmIG film (12 nm), the resonance field (H_{res}) of TmIG (12 nm)/Bi_2Se_3 (6 nm) decreases from 3819 Oe to 3647 Oe. In previous studies on proximity interaction between TmIG (YIG) and TI layers, there is no evidence that the saturated magnetization of TmIG or YIG is changed after the deposition of TI layers,[7–9,11] which can be ascribed to the following reasons: (1) TmIG films were prepared at 800 °C, while Bi_2Se_3 was deposited at 250 °C. This remarkable temperature difference guarantees the stability of the TmIG films and prevents serious intermixing across the interface.[8] (2) The interaction between TmIG and Bi_2Se_3 is of the van der Waals type, in which the mutual epitaxial condition is absent. Thus, the strain and strain-induced anisotropy can be neglected.[7,8] (3) The magnetic moments induced by magnetic proximity effect are unlikely to emerge in Bi_2Se_3 in the temperature range 200–300 K.[12] Therefore, in our experiment, the saturated magnetization of the TmIG films is considered to be unchanged after the growth of the Bi_2Se_3 layer as well. The significant negative shift of H_{res} can be attributed to the interfacial exchange coupling between the spins of TmIG and the exotic TSSs within Bi_2Se_3.[7–9,11] In comparison, it is noted that the H_{res} of TmIG with a Pt (6 nm) capping layer increases slightly from 3819 Oe to 3879 Oe (Fig. 2(a)). The obviously different change of H_{res} is consistent with previous report,[11] which reflects a particular influence of the TI surface states on the magnetic anisotropy of TmIG beyond the strong SOC exhibiting in both Bi_2Se_3 and Pt.

To quantitatively determine the variation of magnetic anisotropy of the TmIG/Bi_2Se_3 films, the FMR measurements were performed as a function of applied field angle (θ_H) with respect to the surface normal direction. Figure 2(b) presents the FMR spectra of TmIG (12 nm)/Bi_2Se_3 (6 nm) measured at different θ_H, which shows that H_{res} increases monotonically as H is rotated from the film normal ($\theta_H = 0°$) to in-plane ($\theta_H = 90°$). Thereafter, the values of H_{res} can be extracted to plot as a function of θ_H, as shown in Fig. 2(c). For a magnetic film with uniaxial PMA, the angular dependent H_{res} can be well fitted as typically done in literature.[13,14] The effective anisotropy field is defined as $4\pi M_{eff} = 4\pi M_s + H_a$, where $4\pi M_s$ and H_a are the demagnetizing field and the uniaxial PMA field, respectively. As a result, it is derived that H_a of the TmIG/Bi_2Se_3 (6 nm) heterostructure increases from 1401 Oe to 1641 Oe by 17.1% relative to bare TmIG, demonstrating the enhanced PMA by the adjacent Bi_2Se_3 layer. Nevertheless, it has been reported recently that the IMA of a 15-nm-thick TmIG film is strengthened after the growth of 7 nm Bi_2Se_3.[11] We speculate that the different growth process of TmIG/Bi_2Se_3 heterostructures and naturally the different interface conditions lead to the discrepancy,[11,15] and such discrepancy has been observed in YIG/Bi_2Se_3 systems, too.[7,9]

To further understand the role of TSSs of Bi_2Se_3 layer in modulating the PMA of TmIG, we systematically investigated the Bi_2Se_3 thickness dependence of H_a of TmIG (12 nm)/Bi_2Se_3 (t_{BS}) in which the surface-to-bulk ratio gradually varied. As shown in Fig. 2(d), it is seen that H_a increases with t_{BS} in the thickness region $0 \leq t_{BS} \leq 6$ nm, and reaches

the maximum at $t_{BS} = 6$ nm. Then, H_a drops with further increasing t_{BS}, even becomes smaller than that of bare TmIG when $t_{BS} \geq 12$ nm. The enhancement of H_a of TmIG should arise from both the strong SOC and the TSSs of the adjacent Bi_2Se_3 layer.[2,6,9,16] While $t_{BS} < 6$ nm, the upper and lower surface states of Bi_2Se_3 with opposite spin polarization directions are coupled by quantum tunneling.[10,17,18] With increasing t_{BS}, the quantum tunneling effect becomes weaker, the spin polarization and SOC of Bi_2Se_3 increase gradually, which gives rise to the enhancement of H_a.[10,18,19] At $t_{BS} = 6$ nm, the opposite spin surface states of the Bi_2Se_3 layer are decoupled, hence H_a reaches the maximum. In the thickness region $t_{BS} > 6$ nm, the H_a of TmIG/Bi_2Se_3 (t_{BS}) decreases with increasing t_{BS}, regardless that the top and bottom surface states of Bi_2Se_3 are decoupled and the spin polarization as well as SOC of Bi_2Se_3 are saturated. As previously reported, the TSSs thickness of Bi_2Se_3 has been estimated to be approximately 2–3 nm.[17,19] Hence, the surface-to-bulk ratio of Bi_2Se_3 decreases with t_{BS}, which resembles the trend of H_a vs. t_{BS} in the region of $t_{BS} > 6$ nm. However, the decline of H_a with t_{BS} cannot simply be ascribed to the decreased weight of TSSs, considering the fact that the reduced H_a of $t_{BS} \geq 12$ nm is even smaller than that of bare TmIG. We speculate that this behavior is originated from the strengthened bulk states of Bi_2Se_3, which become comparable with the surface states of Bi_2Se_3 with further increasing t_{BS}.[20] As a consequence, the PMA of TmIG is modulated by the competition between TSSs and thickness dependent bulk states of Bi_2Se_3 at the interface.

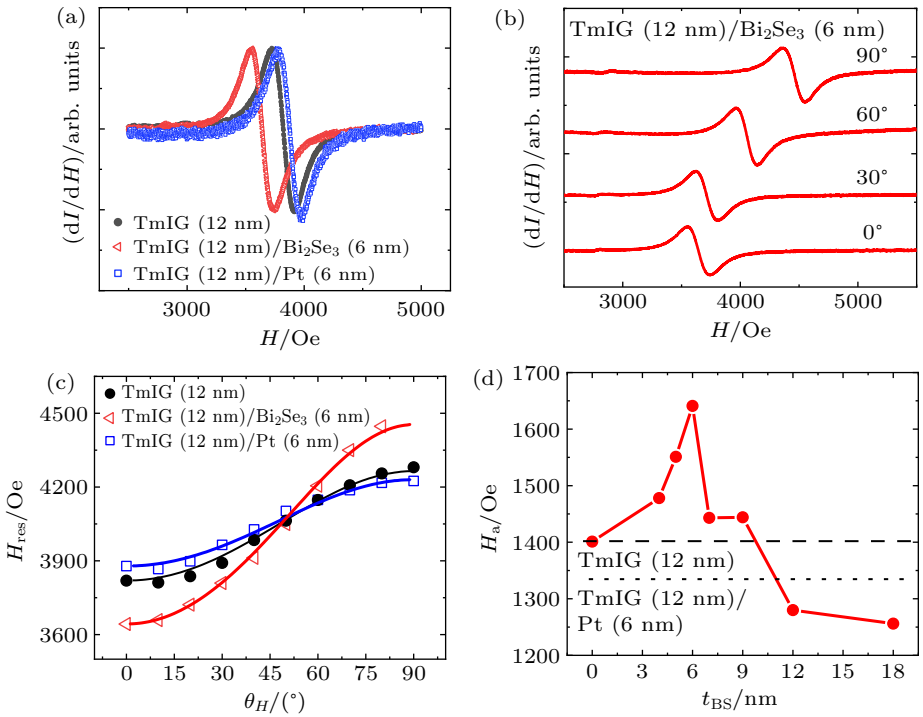


Fig. 2. (a) FMR derivative absorption spectra of TmIG (12 nm), TmIG (12 nm)/Bi_2Se_3 (6 nm), and TmIG (12 nm)/Pt (6 nm) with out-of-plane applied magnetic fields. (b) FMR spectra of TmIG (12 nm)/Bi_2Se_3 (6 nm) as H is rotated from the film normal ($\theta_H = 0°$) to in-plane ($\theta_H = 90°$). (c) θ_H dependence of H_{res} for TmIG (12 nm),TmIG (12 nm)/Bi_2Se_3 (6 nm), and TmIG (12 nm)/Pt (6 nm). The points are experimental data and the solid lines represent the theoretical fit. (d) The t_{BS} dependence of H_a for TmIG (12 nm)/Bi_2Se_3(t_{BS}) heterostructures. The upper and lower dashed lines show the H_a values of TmIG (12 nm) and TmIG (12 nm)/Pt (6 nm), respectively.

3.2. Temperature dependence study

Since the TSSs and bulk states of Bi_2Se_3 may manifest different temperature dependence,[21] we carried out the temperature dependent FMR measurements of TmIG/Bi_2Se_3 heterostructures to further explore the role of TSSs and bulk states of TI in modulating the magnetic anisotropies of TmIG. The FMR spectra of TmIG/Bi_2Se_3 were taken in the temperature range 200–300 K, and the corresponding H_a of TmIG/Bi_2Se_3 as a function of temperature is illustrated in Fig. 3(a). Below 200 K, the FMR signal was too weak to measure due to an insufficient signal-to-noise ratio. It is noted that H_a of TmIG/Bi_2Se_3 (6 nm) rises monotonously as temperature decreases, and H_a of bare TmIG, TmIG/Bi_2Se_3 (12 nm), and TmIG/Pt (6 nm) also shows the similar trend. These characteristics reveal that the strain-induced magnetic anisotropy in TmIG/GGG makes a dominant contribution to the temperature dependence of H_a rather than that of interfacial coupling from the adjacent Bi_2Se_3 layer.[22] Meanwhile, the similar temperature dependence of H_a of TmIG with different Bi_2Se_3 capping layer thickness suggests that the contribution of the TSSs and bulk states of Bi_2Se_3 to PMA of TmIG remains the same within the temperature range of measurement, in consistent with previous reports.[21,23] Furthermore, compared with that of other heterostructures, H_a of TmIG/Bi_2Se_3 (6 nm) ex-

hibits a pronounced enhancement in the measured temperature range. This result confirms that the exchange coupling between Bi_2Se_3 (6 nm) and TmIG is stronger than that of other Bi_2Se_3 thickness, as depicted in Fig. 2(d).

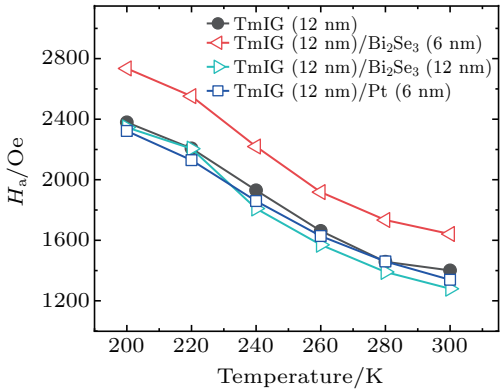


Fig. 3. Temperature dependence of H_a for TmIG (12 nm), TmIG (12 nm)/Bi_2Se_3 (6 nm), TmIG (12 nm)/Bi_2Se_3 (12 nm), and TmIG (12 nm)/Pt (6 nm), respectively.

4. Discussion

For the in-plane magnetized film, such as YIG, the influence of interfacial exchange interaction arising from the adjacent TI layer on its magnetic properties has been discussed previously. Fanchiang *et al.* have observed the enhanced IMA in YIG/Bi_2Se_3, which is attributed to the strengthened exchange coupling between Fe^{3+} ions of YIG mediated by TSS electrons in Bi_2Se_3.[7] In contrast, it is believed that a direct exchange coupling between spins of YIG and TSSs in $(Bi_xSb_{1-x})_2Te_3$ contributes to the strengthened IMA of YIG/$(Bi_xSb_{1-x})_2Te_3$.[8] In our experiments of TmIG/Bi_2Se_3 heterostructures, the modification of PMA can be attributed to the strengthened exchange coupling between Fe^{3+} ions of TmIG mediated by TSS electrons based on the following discussion: (i) The Tm 4f orbitals of TmIG are strongly localized relative to the Fe 3d orbital, hence the Fe^{3+} ions of TmIG are supposed to interact with TSS electrons of Bi_2Se_3.[12,24] Meanwhile, the perpendicular magnetic components of TSS are unlikely to emerge in the TmIG/Bi_2Se_3 heterostructures in the temperature range of 200–300 K,[12] indicating that the spins of TSS of Bi_2Se_3 remain orthogonal to those of Fe^{3+} ions of TmIG. Thus the Heisenberg-like interaction, which may exist at the interface of the YIG/TI heterostructure, can be neglected in the case of TmIG/Bi_2Se_3. (ii) It has been reported that the interfacial Dzyaloshinskii–Moriya interaction (DMI) can produce magnetic skyrmions in TmIG/Pt heterostructures at elevated temperatures, which generates the topological Hall effect.[25] However, such effect has not been observed in TmIG/Bi_2Se_3 system so far,[11,26] implying that the interfacial DMI is not responsible for the TSSs modulated PMA of TmIG films. (iii) Recently, it has been experimentally indicated that the EuS/Bi_2Se_3 system exhibits a largely enhanced Curie temperature and PMA.[2] Kim *et al.* has demonstrated theoretically that the proximity effect of TSSs results in PMA of EuS, and the large exchange coupling between Eu atoms is mediated by the highly coherent TSSs through the Ruderman–Kittel–Kasuya–Yosida (RKKY) type interactions.[6] Therefore, we ascribe the modification of PMA in TmIG/Bi_2Se_3 to the strengthened exchange coupling between Fe^{3+} ions mediated by TSS electrons via the RKKY type interaction.

5. Conclusion and perspectives

In summary, the magnetic anisotropy of TmIG under the influence of adjacent Bi_2Se_3 layers has been investigated. The PMA of TmIG can be greatly enhanced by the Bi_2Se_3 layer via interfacial coupling. Through the Bi_2Se_3 thickness dependence study, we reveal that the competition between TSSs and thickness dependent bulk states of Bi_2Se_3 gives rise to the modulation of PMA of the Bi_2Se_3/TmIG heterostructures. The interfacial interaction can be attributed to the enhanced exchange coupling between Fe^{3+} ions of TmIG mediated by TSS electrons of Bi_2Se_3. Our results provide useful references for future work on the exploitation of FMI/TI based spintronic devices.

References

[1] Qi X L and Zhang S C 2011 *Rev. Mod. Phys.* **83** 1057
[2] Katmis F, Lauter V, Nogueira F S, Assaf B A, Jamer M E, Wei P, Satpati B, Freeland J W, Eremin I, Heiman D, Jarillo-Herrero P and Moodera J S 2016 *Nature* **533** 513
[3] Li M, Song Q, Zhao W, Garlow J A, Liu T H, Wu L, Zhu Y, Moodera J S, Chan M H W, Chen G and Chang C Z 2017 *Phys. Rev. B* **96** 201301
[4] Watanabe R, Yoshimi R, Kawamura M, Mogi M, Tsukazaki A, Yu X Z, Nakajima K, Takahashi K S, Kawasaki M and Tokura Y 2019 *Appl. Phys. Lett.* **115** 102403
[5] Qi X L, Hughes T L and Zhang S C 2008 *Phys. Rev. B* **78** 195424
[6] Kim J, Kim K W, Wang H, Sinova J and Wu R 2017 *Phys. Rev. Lett.* **119** 027201
[7] Fanchiang Y T, Chen K H M, Tseng C C, Chen C C, Cheng C K, Yang S R, Wu C N, Lee S F, Hong M and Kwo J 2018 *Nat. Commun.* **9** 223
[8] Tang C, Song Q, Chang C Z, Xu Y, Ohnuma Y, Matsuo M, Liu Y, Yuan W, Yao Y, Moodera J S, Maekawa S, Han W and Shi J 2018 *Sci. Adv.* **4** eaas8660
[9] Liu T, Kally J, Pillsbury T, Liu C, Chang H, Ding J, Cheng Y, Hilse M, Engel-Herbert R, Richardella A, Samarth N and Wu M 2020 *Phys. Rev. Lett.* **125** 017204
[10] Landolt G, Schreyeck S, Eremeev S V, Slomski B, Muff S, Osterwalder J, Chulkov E V, Gould C, Karczewski G, Brunner K, Buhmann H, Molenkamp L W and Dil J H 2014 *Phys. Rev. Lett.* **112** 057601
[11] Chen C C, Chen K H M, Fanchiang Y T, Tseng C C, Yang S R, Wu C N, Guo M X, Cheng C K, Huang S W, Lin K Y, Wu C T, Hong M and Kwo J 2019 *Appl. Phys. Lett.* **114** 031601
[12] Yang C Y, Lee Y H, Ou Yang K H, Chiu K C, Tang C, Liu Y, Zhao Y F, Chang C Z, Chang F H, Lin H J, Shi J and Lin M T 2019 *Appl. Phys. Lett.* **114** 082403
[13] Makino H and Hidaka Y 1981 *Mater. Res. Bull.* **16** 957
[14] Kakazei G N, Wigen P E, Guslienko K Y, Chantrell R W, Lesnik N A, Metlushko V, Shima H, Fukamichi K, Otani Y and Novosad V 2003 *J. Appl. Phys.* **93** 8418
[15] Wu C N, Tseng C C, Lin K Y, Cheng C K, Yeh S L, Fanchiang Y T, Hong M and Kwo J 2018 *AIP Adv.* **8** 055904
[16] Semenov Y G, Duan X and Kim K W 2012 *Phys. Rev. B* **86** 161406

[17] Zhang Y, He K, Chang C Z, Song C L, Wang L L, Chen X, Jia J F, Fang Z, Dai X, Shan W Y, Shen S Q, Niu Q, Qi X L, Zhang S C, Ma X C and Xue Q K 2010 *Nat. Phys.* **6** 584

[18] Neupane M, Richardella A, Sánchez-Barriga J, Xu S, Alidoust N, Belopolski I, Liu C, Bian G, Zhang D, Marchenko D, Varykhalov A, Rader O, Leandersson M, Balasubramanian T, Chang T R, Jeng H T, Basak S, Lin H, Bansil A, Samarth N and Hasan M Z 2014 *Nat. Commun.* **5** 1

[19] Wang H, Kally J, Lee J S, Liu T, Chang H, Hickey D R, Mkhoyan K A, Wu M, Richardella A and Samarth N 2016 *Phys. Rev. Lett.* **117** 076601

[20] Taskin A A, Sasaki S, Segawa K and Ando Y 2012 *Phys. Rev. Lett.* **109** 066803

[21] He L, Xiu F, Yu X, Teague M, Jiang W, Fan Y, Kou X, Lang M, Wang Y, Huang G, Yeh N C and Wang K L 2012 *Nano Lett.* **12** 1486

[22] Quindeau A, Avci C O, Liu W, Sun C, Mann M, Tang A S, Onbasli M C, Bono D, Voyles P M, Xu Y, Robinson J, Beach G S D and Ross C A 2017 *Adv. Electron. Mater.* **3** 1600376

[23] Wang Y, Deorani P, Banerjee K, Koirala N, Brahlek M, Oh S and Yang H 2015 *Phys. Rev. Lett.* **114** 257202

[24] Shao Q, Grutter A, Liu Y, Yu G, Yang C Y, Gilbert D A, Arenholz E, Shafer P, Che X, Tang C, Aldosary M, Navabi A, He Q L, Kirby B J, Shi J and Wang K L 2019 *Phys. Rev. B* **99** 104401

[25] Shao Q, Liu Y, Yu G, Kim S K, Che X, Tang C, He Q L, Tserkovnyak Y, Shi J and Wang K L 2019 *Nat. Electron.* **2** 182

[26] Yang S R, Fanchiang Y T, Chen C C, Tseng C C, Liu Y C, Guo M X, Hong M, Lee S F and Kwo J 2019 *Phys. Rev. B* **100** 045138